The 2nd Joint International Conference on Multibody System Dynamics
May 29–June 1, 2012, Stuttgart, Germany

Analytic Solution to 3-Dimensional, Single Point Collision Problems Using Stronge's Hypothesis

Adrian Rodriguez*, **Alan Bowling***

* Department of Mechanical and Aerospace Engineering
University of Texas at Arlington
Box 19023, 500 W. First Street, Arlington, TX 76019, USA
adrianrodriguez2009@mavs.uta.edu, bowling@uta.edu

ABSTRACT

This work presents a unique algorithm to obtain an analytic solution to the post-impact behavior of three-dimensional (3D) rigid body collision problems. The proposed method is developed to address the issues which arise in the sticking region for single point impact with friction. Stronge's hypothesis, which incorporates the principles of the work-energy theorem is used to treat the energy lost during the rigid body collision. A discrete, algebraic modeling approach is used with an event-driven function which finds impact events. Coulomb friction is used to describe the relationship between the normal and tangential impulses. A benchmark example is considered to evaluate the effectiveness of the proposed algorithm.

1 INTRODUCTION

The most common characteristics of impacts, which occur over a very short time period, are rapid velocity changes and the presence of large forces on the bodies [12]. Here, the detection of an impact is captured using an event function in conjunction with Matlab's ode45.m integrator. It is assumed that the position and orientation of the system remains constant throughout the collision [7].

The rigid body impacts are modeled as discrete events using a discontinuous approach, also termed as piecewise [8], nonsmooth [7], or impact and continuous [17]. This approach characterizes the collisions as "hard" impacts, involving an instantaneous change in the velocities of the impacting bodies [3, 4]. The large impact forces are generated by very small local deformations when a rigid body impact is assumed [18]. Unilateral constraints are included in the model to avoid penetration and normal compliance between the impacting bodies [14, 15]. In contrast, continuous modeling approaches, also known in the literature as regularized [8], non-colliding [17], or compliant [7] contact force models often involve penalty methods and complementarity formulations. These models incorporate the properties of stiff springs and dampers to model the impact which may allow for the existence of small local deformations between the impacting bodies. A relationship between the local deformations and the time-varying forces on the bodies is established [7, 10, 13].

The collision is treated as continuous in this work and examined in the impulse-domain [18]. An analytic solution similar to [5] which considers the system's energy is implemented for three-dimensional, single point impact. The energy dissipated at impact is defined by a hypothesis which describes the system's momenta before and after impact. Classical hypotheses include Newton's (velocities), Poisson's (impulses), and Stronge's (energy); each one uniquely defines a coefficient of restitution and are commonly used to examine hard impacts. Stronge's hypothesis defines an energetic coefficient of restitution which makes use of the work-energy theorem, as in [1, 18], and is accepted as the most energetically consistent approach to impact modeling. The application of an analytic approach for planar problems is well documented in the literature, [5, 16], but has proven difficult for the three-dimensional case. The main difficulty lies in the

region of no-slip, or sticking on the impact plane where the direction of friction is unknown. The complex nature of friction makes it difficult to predict its behavior in the sticking region, as noted in [12]. Partial analytic approaches to these problems were proposed but implemented numerical integration techniques for solving these problems, [1, 2].

In this work, a complete analytic approach is developed which addresses the issues that arise in the sticking region for three-dimensional collision problems. An algorithm is constructed, which first plots the normal and tangential velocities of the impact points as a function of the normal impulse throughout the collision. This is accomplished by expressing the system equations of motion in a form that relates the instantaneous spatial velocities to the normal impulse. The ambiguity of the friction direction in the sticking region is resolved by using the system equations of motion to map the value of the tangential impulses. This provides knowledge about the friction direction and the paths of the tangential velocities when slipping resumes. The remainder of the algorithm uses work-energy theory and Stronge's energetic coefficient of restitution to determine the normal impulse at the collision end. The incorporation of Stronge's hypothesis provides the basis for examining three-dimensional, single point collision problems with friction, which leads to a unique and energetically consistent solution. The velocities at the end of the collision are calculated, which dictate the post-impact behavior of the system considered.

The remainder of the paper is organized as follows. The parts of the algorithm, which uses an analytic approach is developed for three-dimensional, single point impact with friction will be discussed in detail. Then, the simulation results of a benchmark example are presented and the paper will end with some meaningful conclusions drawn from this work.

2 THREE-DIMENSIONAL IMPACT

In this section, the equations of motion are first rewritten and expressed in terms of the normal impulse parameter. Then, a discussion about the issues that arise in the sticking region and how it is addressed in this work is presented.

2.1 Equations of motion

The equations of motion, which are derived using Kane's method [11], take the form of

$$M\ \ddot{\mathbf{q}} + \mathbf{g}(\mathbf{q}) \ = \ \mathbf{\Gamma}(\mathbf{q}) \ = \ J^T(\mathbf{q})\ \mathbf{F} \tag{1}$$

where M is the mass matrix, $\mathbf{\Gamma}$ contains the generalized active forces, and J is a Jacobian matrix that defines the velocity and forces at the impact points. The generalized coordinates and accelerations are included in $\mathbf{q}$ and $\ddot{\mathbf{q}}$, while $\mathbf{g}$ and $\mathbf{F}$ are vectors of gravity and impact forces, respectively.

A definite integration of (1) over a short time ϵ for the impact event,

$$\int_t^{t+\epsilon} \left(M\ \ddot{\mathbf{q}} + \mathbf{g}\ (\mathbf{q})\right)\ dt = \int_t^{t+\epsilon} J^T(\mathbf{q})\ \mathbf{F}\ dt \tag{2}$$

yields,

$$M\ (\ \dot{\mathbf{q}}(t+\epsilon) - \dot{\mathbf{q}}(t)\ ) = J^T\mathbf{p} \tag{3}$$

Multiplying the inverse of the mass matrix on each side and using $\triangle\dot{\mathbf{q}}$ to represent the change between pre and post-impact generalized speeds,

$$\triangle\dot{\mathbf{q}} = M^{-1}J^T\mathbf{p} = \mathrm{L}\ \mathbf{p} = [\mathbf{L}_{t1} \mid \mathbf{L}_{t2} \mid \mathbf{L}_n]\ \ \mathbf{p} \tag{4}$$

where $\mathrm{L} \in \Re^{3X3}$ can be termed as a collision matrix. The columns of L are shown to uncover their respective normal and tangential contributions as column vectors. Finally, the product can be carried out such that the

equations of motion take the form of,

$$\triangle\dot{\mathbf{q}} = \mathbf{L}_{t1}\, p_{t1} + \mathbf{L}_{t2}\, p_{t2} + \mathbf{L}_n\, p_n \tag{5}$$

In this work, Coulomb friction is used to characterize the relationship between normal and tangential forces using a coefficient of friction μ,

$$\mathbf{f}_t = \pm\mu\, |f_n| \tag{6}$$

where the sign in (6) will depend on the direction of friction at the impact point. Given that the method used here considers the impulses at impact, (6) can be expressed in terms of impulses as in [6, 9] after a definite integration,

$$\mathbf{p}_t = \pm\mu\, |p_n| \tag{7}$$

The absolute value of the normal impulse term in (5) can be taken while preserving its sign and the Coulomb friction relationship in (7) can be substituted using velocity components to give,

$$\triangle\dot{\mathbf{q}} = \mathbf{L}_{t1}\left(\pm\mu\frac{v_{t1}}{\sqrt{{v_{t1}}^2 + {v_{t2}}^2}}\right)|p_n| + \mathbf{L}_{t2}\left(\pm\mu\frac{v_{t2}}{\sqrt{{v_{t1}}^2 + {v_{t2}}^2}}\right)|p_n| + \mathbf{L}_n|p_n| \tag{8}$$

where the sign of the tangential terms are kept ambiguous and will depend on the direction of friction acting at the impact point. The coefficients of the normal impulse term in (8) can be collected to obtain,

$$\triangle\dot{\mathbf{q}} = \left(\mathbf{L}_n \pm \mu\left[\left(\frac{v_{t1}}{\sqrt{{v_{t1}}^2 + {v_{t2}}^2}}\right)\mathbf{L}_{t1} + \left(\frac{v_{t2}}{\sqrt{{v_{t1}}^2 + {v_{t2}}^2}}\right)\mathbf{L}_{t2}\right]\right)|p_n| \tag{9}$$

It is clear from (9) that the use of Coulomb friction to represent the direction of the tangential impulses, fails in the sticking region (ie. when $\mathbf{v}_t = 0$, such that $v_{t1} = v_{t2} = 0$), as noted in [1, 2]. If only one of the tangential components is zero, then (9) is still applicable and the system behaves similar to a planar impact problem. The situation in which the impact point reaches the sticking region and(9) cannot be used is addressed in the following section.

The expression in (9) also describes the dependence of the post-impact generalized speeds in $\dot{\mathbf{q}}$ on the normal impulse, $|p_n|$, since $\triangle\dot{\mathbf{q}} = \dot{\mathbf{q}} - \dot{\mathbf{q}}_o$. The duality of the impact Jacobian which expresses a relationship between velocities and forces, shown as

$$\boldsymbol{\vartheta} = \begin{bmatrix} v_{t1} \\ v_{t2} \\ v_n \end{bmatrix} = J\,\dot{\mathbf{q}}\,, \qquad \boldsymbol{\Gamma} = J^T\,\mathbf{F} = J^T \begin{bmatrix} f_{t1} \\ f_{t2} \\ f_n \end{bmatrix} \tag{10}$$

such that the left-hand side of (9) can be written as,

$$\triangle\dot{\mathbf{q}} \;= \dot{\mathbf{q}} - \dot{\mathbf{q}}_o = (J^T J)^{-1} J^T J(\dot{\mathbf{q}} - \dot{\mathbf{q}}_o) = (J^T J)^{-1} J^T(\boldsymbol{\vartheta} - \boldsymbol{\vartheta}_o) = J^*(\boldsymbol{\vartheta} - \boldsymbol{\vartheta}_o) \tag{11}$$

Equating (11) back with the right-hand side of (9) yields,

$$J^*(\boldsymbol{\vartheta} - \boldsymbol{\vartheta}_o) = \mathbf{L}\,|p_n| \tag{12}$$

where it is clearer to see the effect of $|p_n|$ on the normal velocities contained in $\boldsymbol{\vartheta}$. In this way, the calculation of the normal work is derived for the application of Stronge's hypothesis which is discussed in Sec. 3.1.

2.2 Sticking region

As it was noted in Sec. 2.1, the use of (9) is not valid if the impact point reaches sticking during the compression phase of the collision. This is problematic because the tangential velocity components go to zero. In order to determine the behavior of the system in the sticking region, some knowledge about the friction direction is needed. If we revisit (3) and multiply the inverse of the mass matrix on each side,

$$\dot{\mathbf{q}}(t+\epsilon) - \dot{\mathbf{q}}(t) = M^{-1}\, J^T \mathbf{p} \tag{13}$$

in which m $\leq$ n making it an underconstrained system of equations. The two unknowns in (13) are $\dot{\mathbf{q}}(t+\epsilon)$ and $\mathbf{p}$. Not all of the terms in $\dot{\mathbf{q}}$ contribute to the impact forces in $\mathbf{p}$. The contributing terms in $\dot{\mathbf{q}}$ can be expressed as the velocities of the impact points using the properties of the impact Jacobian in (10),

$$\boldsymbol{\vartheta}(t+\epsilon) - \boldsymbol{\vartheta}(t) = J\, M^{-1}\, J^T \mathbf{p} \tag{14}$$

resulting in a one-to-one mapping between the velocities and forces involved at impact. Solving for $\mathbf{p}$ gives,

$$\left(JM^{-1}J^T\right)^{-1} \left(\boldsymbol{\vartheta}(t+\epsilon) - \boldsymbol{\vartheta}(t)\right) = \left(JM^{-1}J^T\right)^{-1} \left(\begin{bmatrix} v_{t1} \\ v_{t2} \\ v_n \end{bmatrix} - \begin{bmatrix} v_{t1_o} \\ v_{t2_o} \\ v_{n_o} \end{bmatrix} \right) = \mathbf{p} \tag{15}$$

The solution of the impulses is dependent on the change between the initial and final components of the spatial velocities of the impact point. For the case of sticking, $v_{t1} = v_{t2}$ = 0 but v_n is not known and is dependent on the amount of energy lost in the collision. If a set of values for v_n from the perfectly elastic (ie. $v_n = -v_{n_o}$) to perfectly plastic (ie. $v_n = 0$) collision cases is assumed, then a corresponding set of impulses for each collision are obtained. The friction direction is determined using the tangential impulses and is plotted as a function of the normal impulse. Since the normal impulse at sticking is known from (9), it is used to find the friction direction from the plot and determine what the subsequent motion of the impact point is after sticking. This process provides the means to model three-dimensional impact problems when sticking is encountered. Its implementation in the analysis is discussed further in Sec. 4.

3 ANALYTIC APPROACH

In this section, the analytic approach is developed for three-dimensional, single point impact. This is followed by the method used to calculate the normal work and application of Stronge's hypothesis.

3.1 Work-Energy Theorem

Here, the derivation of the normal work resulting from the rigid body collision will be developed. As it was noted earlier, an energetic COR according to Stronge's hypothesis [18] is used in this work to treat the rigid body impact.

Stronge's hypothesis incorporates the work-energy theorem by relating the normal work between the compression and restitution phases of the collision. The work-energy theorem defines that the sum of the final kinetic, T_f, and potential, U_f, energy of a system is equal to the sum of the initial kinetic, T_o, and potential, U_o, energy plus the work done, W, to get to the final state. This can be written for the rigid body collision considered here as,

$$T_f = T_o + W \tag{16}$$

where the potential energy terms have been neglected due to the hard impact modeling used. The calculation of the work is given as the change in kinetic energy between the final and initial states of the collision as,

$$W = T_f - T_o = \frac{1}{2}\, \dot{\mathbf{q}}^T M\, \dot{\mathbf{q}} - \frac{1}{2}\, \dot{\mathbf{q}}_o^T M\, \dot{\mathbf{q}}_o \tag{17}$$

By using the same representation of the generalized speeds $\dot{\mathbf{q}}$ and $\dot{\mathbf{q}}_o$ in (11), then (17) can be expressed as,

$$W = \frac{1}{2}\,(J^*\boldsymbol{\vartheta})^T M\,(J^*\boldsymbol{\vartheta}) - \frac{1}{2}\,(J^*\boldsymbol{\vartheta}_o)^T M\,(J^*\boldsymbol{\vartheta}_o) \tag{18}$$

where the velocities at the impact points in $\boldsymbol{\vartheta}$ and $\boldsymbol{\vartheta}_o$ can be realized in the calculation of the work.

$$W = \frac{1}{2}\left(J^*\begin{bmatrix} v_{t1} \\ v_{t2} \\ v_n \end{bmatrix}\right)^T M \left(J^*\begin{bmatrix} v_{t1} \\ v_{t2} \\ v_n \end{bmatrix}\right) - \frac{1}{2}\left(J^*\begin{bmatrix} v_{t1} \\ v_{t2} \\ v_n \end{bmatrix}_o\right)^T M \left(J^*\begin{bmatrix} v_{t1} \\ v_{t2} \\ v_n \end{bmatrix}_o\right) \tag{19}$$

Stronge's hypothesis only considers the normal work done during a collision which is a function of the normal velocity of the impact point. To capture the effects that the right hand side of (19) has on the normal work due to the normal velocity, then a distinction must be made between the contributing and non-contributing parts.

If the term J^* is split into column vectors and represented as $J^* = [\mathbf{J}_1^*|\mathbf{J}_2^*|\mathbf{J}_3^*]$, then the product of these vectors with the velocity components in (19) yields,

$$W = \frac{1}{2}\,(\mathbf{J}_t^*\boldsymbol{\vartheta}_t + \mathbf{J}_n^*\boldsymbol{\vartheta}_n)^T M\,(\mathbf{J}_t^*\boldsymbol{\vartheta}_t + \mathbf{J}_n^*\boldsymbol{\vartheta}_n) - \frac{1}{2}\,(\mathbf{J}_t^*\boldsymbol{\vartheta}_{t_o} + \mathbf{J}_n^*\boldsymbol{\vartheta}_{n_o})^T M\,(\mathbf{J}_t^*\boldsymbol{\vartheta}_{t_o} + \mathbf{J}_n^*\boldsymbol{\vartheta}_{n_o}) \tag{20}$$

where $\mathbf{J}_t^* = [\mathbf{J}_1^*|\mathbf{J}_2^*]$ and $\mathbf{J}_n^* = [\mathbf{J}_3^*]$. The normal and tangential velocity components in (20) are distinguished by the terms $\boldsymbol{\vartheta}_t = [v_{t1}|v_{t2}]^T$ and $\boldsymbol{\vartheta}_n = [v_n]$, respectively. The product of the terms in (20) can be carried out to determine the location of the normal velocity term with respect to the tangential terms so that only the parts contributing to the normal work can be extracted.

$$\begin{aligned} W = {} & \frac{1}{2}(\boldsymbol{\vartheta}_t^T\mathbf{J}_t^{*T} M\,\mathbf{J}_t^*\boldsymbol{\vartheta}_t + 2\,\boldsymbol{\vartheta}_t^T\mathbf{J}_t^{*T} M\,\mathbf{J}_n^*\boldsymbol{\vartheta}_n + \boldsymbol{\vartheta}_n\mathbf{J}_n^{*T} M\,\mathbf{J}_n^*\boldsymbol{\vartheta}_n) \\ & - \frac{1}{2}(\boldsymbol{\vartheta}_{t_o}^T\mathbf{J}_t^{*T} M\,\mathbf{J}_t^*\boldsymbol{\vartheta}_{t_o} + 2\,\boldsymbol{\vartheta}_{t_o}^T\mathbf{J}_t^{*T} M\,\mathbf{J}_n^*\boldsymbol{\vartheta}_{n_o} + \boldsymbol{\vartheta}_{n_o}\mathbf{J}_n^{*T} M\,\mathbf{J}_n^*\boldsymbol{\vartheta}_{n_o}) \end{aligned} \tag{21}$$

A careful look at all the parts in (21) shows tangential, normal, and coupled tangential and normal parts, and are represented by the $\boldsymbol{\vartheta}_t$ and $\boldsymbol{\vartheta}_n$ terms. As it was stated earlier, the normal velocity at the impact point is the primary source to the normal work done in the collision. Thus, if the tangential parts are neglected and only the parts that are a function of the normal velocity, in $\boldsymbol{\vartheta}_n$, are considered, then the normal work can be expressed as,

$$W_n = (\boldsymbol{\vartheta}_t^T\mathbf{J}_t^{*T} M\,\mathbf{J}_n^*\boldsymbol{\vartheta}_n + \frac{1}{2}\boldsymbol{\vartheta}_n\mathbf{J}_n^{*T} M\,\mathbf{J}_n^*\boldsymbol{\vartheta}_n) - (\boldsymbol{\vartheta}_{t_o}^T\mathbf{J}_t^{*T} M\,\mathbf{J}_n^*\boldsymbol{\vartheta}_{n_o} + \frac{1}{2}\boldsymbol{\vartheta}_{n_o}\mathbf{J}_n^{*T} M\,\mathbf{J}_n^*\boldsymbol{\vartheta}_{n_o}) \tag{22}$$

3.2 Stronge's hypothesis for 3D single point impact

A plot of the normal work for a rigid body collision, as in Fig. 1, shows its quadratic nature as a function of $|p_n|$. The minima from the curve at $|p_{nc}|$ marks the end of the work done in the compression phase, W_{nc}, and the start of the restitution phase. This point can be solved for by differentiating (22) with respect to the normal impulse, $|p_n|$, and equating it to zero.

The compression phase end is also noted under Stronge's hypothesis to occur when the normal velocity reaches zero for single point impact. A different approach to the calculation of work, as in [1], is presented to show how Stronge's hypothesis can be interpreted for the case of three-dimensional, single point impact.

Consider work during the collision to be the integration of the dot product between force and displacement, such that

$$W = \int \mathbf{F}\cdot d\mathbf{x} = \int \mathbf{F}\cdot d(x_{t1}\,\mathbf{N}_1 + x_{t2}\,\mathbf{N}_2 + x_n\,\mathbf{N}_3) \tag{23}$$

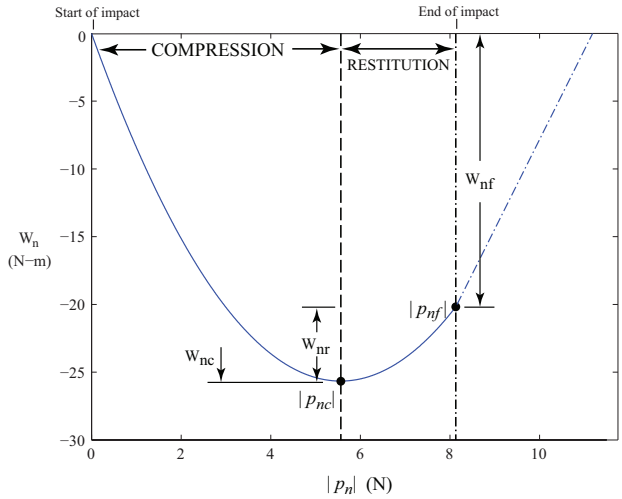

Figure 1. Plot of W_n vs. $|p_n|$ for a rigid body collision.

where $\mathbf{F}$ contains the vector representations for normal and tangential forces at the impact point. The normal work can be expressed as,

$$W_n = \int f_n \, dx_n \tag{24}$$

From (24), the normal forces can be written as the time differentiation of the normal impulse which gives,

$$W_n = \int dp_n \frac{dx_n}{dt} = \int v_n \, dp_n = \int v_n \, d|p_n| \tag{25}$$

where the absolute value of the normal impulse is taken and the signs are preserved as in (8), consistent with the formulation presented in Sec. 2.1. The significance of the normal velocity is apparent from (25) in the determination of the normal work during the collision. The differentiation of (25) with respect to $|p_n|$ gives the compression phase end, which occurs when the normal velocity reaches zero.

$$\frac{dW_n}{d|p_n|} = v_n = 0 \tag{26}$$

The result in (26) provides a generalized interpretation of Stronge's hypothesis for the consideration of three-dimensional impact. The net normal work, W_{nf}, at the end of the collision is determined using Stronge's hypothesis which is defined as [18],

$$e_*^2 = -\frac{W_{nr}}{W_{nc}} = -\frac{W_{nf} - W_{nc}}{W_{nc}} \tag{27}$$

such that,

$$W_{nf} = W_{nc}(1 - e_*^2) \tag{28}$$

where $0 \leq e_* \leq 1$ and W_{nr} is the normal work done during the restitution phase of the collision. The normal impulse, $|p_{nf}|$ shown in Fig. 1, signifies the end condition for the collision and can be determined once W_{nf} is known.

4 RESULTS

4.1 Benchmark example: double pendulum

A double pendulum, shown in Fig. 2, is considered as a benchmark example to demonstrate the effectiveness of the proposed approach. The system is composed of two bodies each with length L and has six degrees-of-freedom (DOFs) described using Euler angles given by generalized coordinates, $\mathbf{q} = \{q_1, \ldots, q_6\}$. At impact with the ground surface, three force components are present at the impact point; one force is normal to both surfaces and the other two are tangential forces on the impact plane, which are caused by friction.

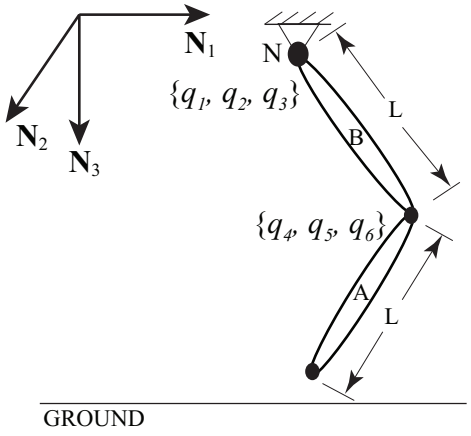

Figure 2. Model description for double pendulum.

The focus of this analysis is to consider the case of sticking for three-dimensional, single point impact. The results of the analysis are presented in Fig. 3. The algorithm first constructs a plot using (9), which shows the evolution of the velocity components in the impulse domain during the collision, as shown in Fig. 3 (a). The tangential components cross the $v = 0$ line at the same point in the compression phase of the collision, which indicates that the impact point reached the sticking region (ie. $\mathbf{v}_t = 0$).

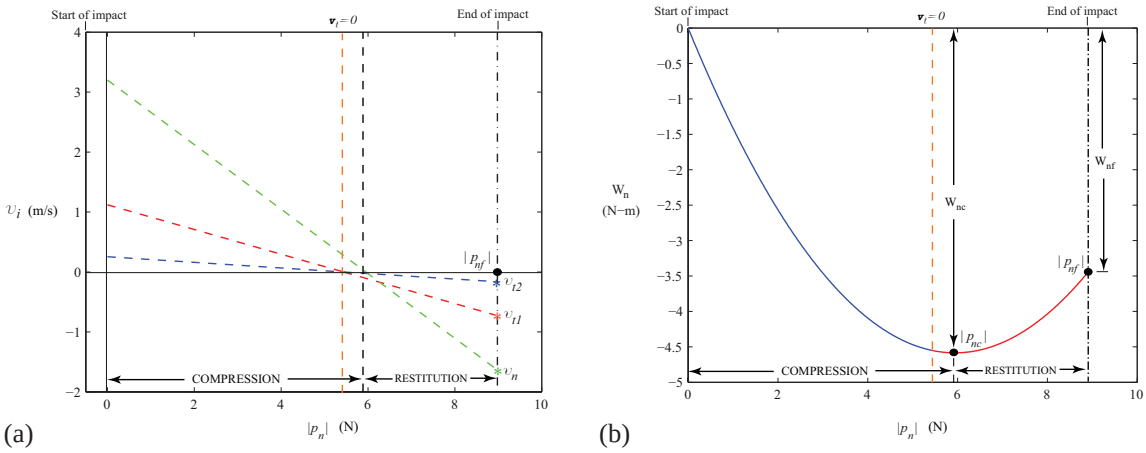

(a) (b)

Figure 3. (a) Velocity paths throughout the collision, (b) Normal work done throughout the collision.

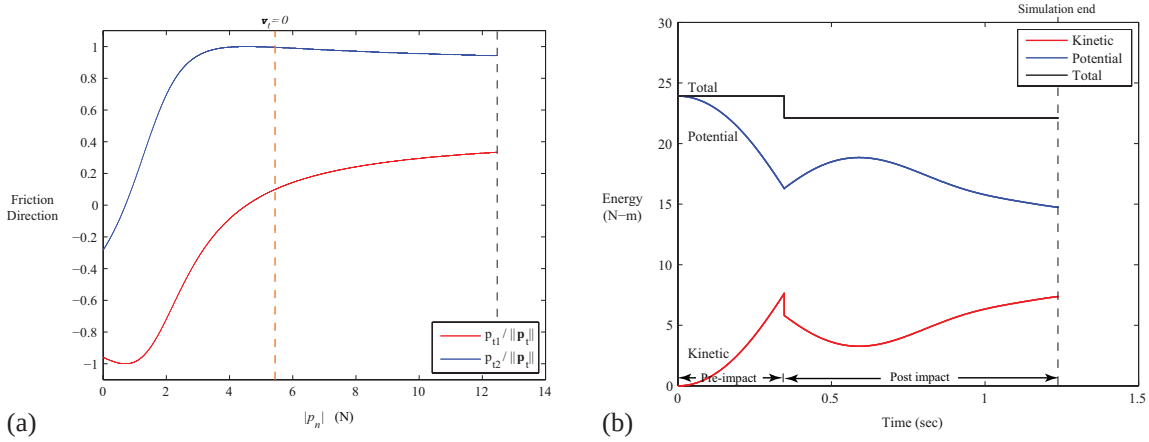

Figure 4. (a) Simulation results for double pendulum, (b) Energy consistency during the simulation.

To address the sticking region, the next phase of the algorithm uses (15) to generate a relationship between the friction direction and the normal impulse of the collision. This is graphically represented in Fig. 4 (a). Recall, values of v_n were varied from perfectly elastic (ie. $v_n = -v_{n_o}$) to perfectly plastic (ie. $v_n = 0$) cases to obtain the curve. The friction direction at the point of sticking is determined using the normal impulse from Fig. 3 (a) when $\mathbf{v}_t = 0$, and locating this point on Fig. 4 (a). The remainder of the analysis is carried out using (9) after sticking. The last phase of the algorithm uses the developments from Sec. 3.1 and 3.2 with the work-energy theorem to construct a plot of the normal work throughout the collision, as seen in Fig. 3 (b). The normal work at the compression phase end, W_{nc}, is used to apply Stronge's hypothesis, and determine the net normal work and normal impulse at the end of the collision. Using (9), the terminal velocities of the impact point are determined for the collision, which is illustrated in Fig. 3 (a).

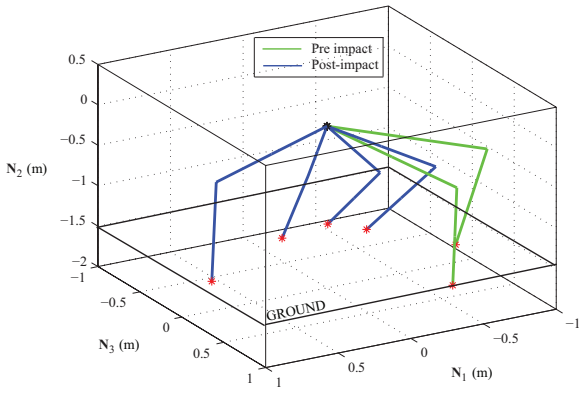

Figure 5. Simulation results for the double pendulum.

A plot of the kinetic, potential, and total energy throughout the simulation is shown in Fig. 4 (b). The total energy remains constant and demonstrates the energy consistency that is maintained in the simulation. A loss of kinetic energy is seen at the point of impact, which is consistent for rigid body collisions; this loss also corresponds to the net normal work, W_{nf}, seen in Fig. 3 (b). The simulation results from the analysis of the double pendulum is illustrated in Fig. 5 and additional planar views are included in Fig. 6. The analysis showed the effectiveness of the proposed approach for three-dimensional, single point impact.

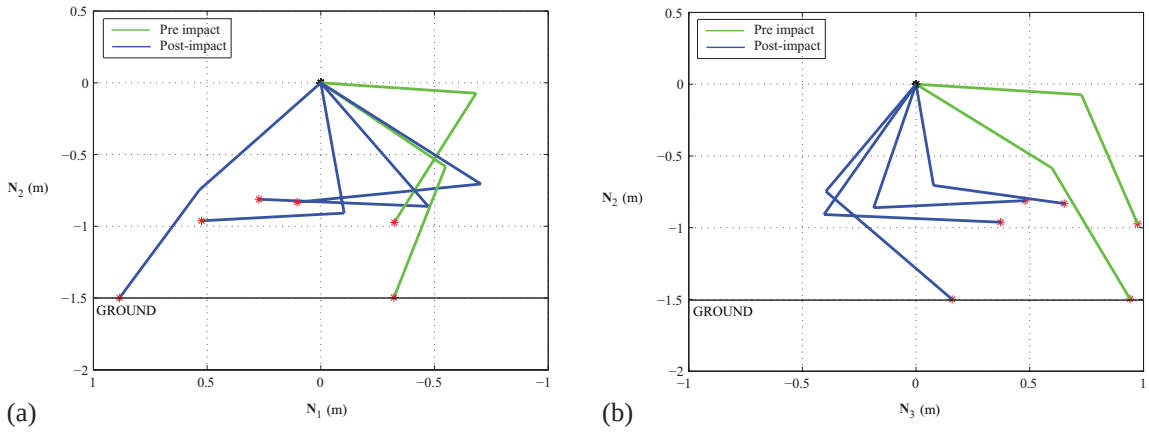

Figure 6. (a) $\mathbf{N}_1 - \mathbf{N}_2$ view of the simulation results, (b) $\mathbf{N}_2 - \mathbf{N}_3$ view of the simulation results.

5 CONCLUSIONS

In this work, an algorithm, which incorporates an analytic approach for three-dimensional, single point impact with friction was developed. A benchmark example was considered here to demonstrate the applicability and effectiveness of the proposed approach. The developments made in this work addressed the region of sticking, which is problematic in three-dimensional impact problems. It was shown that the algorithm made it feasible to obtain an analytic solution to the post-impact generalized speeds of the system. It was also shown that the solution was energetically consistent by using the proposed approach to treat the rigid body collision.

REFERENCES

[1] P. Bergés and A. Bowling. Rebound, slip, and compliance in the modeling and analysis of discrete impacts in legged locomotion. *Jour. of Vibration and Control*, 17(12):1407–1430, December 2006.

[2] V. Bhatt and J. Koechling. Three-dimensional frictional rigid-body impact. *Journal of Appl. Mech.*, 62:893–897, December 1995.

[3] S. Djerassi. Collision with friction; part A: Newton's hypothesis. *Multibody System Dynamics*, 21(1):37–54, February 2009.

[4] S. Djerassi. Collision with friction; part B: Poisson's and stronge's hypotheses. *Multibody Sys Dyn*, 21(1):55–70, February 2009.

[5] S. Djerassi. Stronge's hypothesis-based solution to the planar collision-with-friction problem. *Multibody System Dynamics*, 24(4):493–515, December 2010.

[6] D.M. Flickinger and A. Bowling. Simultaneous oblique impacts and contacts in multibody systems with friction. *Multibody System Dynamics*, 23(3):249–261, March 2010.

[7] G. Gilardi and I. Sharf. Literature survey of contact dynamics modeling. *Mechanism and Machine Theory*, 37(10):1213–1239, October 2002.

[8] Y. Gonthier, J. McPhee, C. Lange, and J-C. Piedboeuf. A regularized contact model with asymmetric damping and dwell-time dependent friction. *Multibody System Dynamics*, 11(3):209–233, April 2004.

[9] I. Han and B.J. Gilmore. Multi-body impact motion with friction-analysis, simulation, and experimental validation. *Journal of Mechanical Design, Transactions of the ASME*, 115(3):412–422, September 1993.

[10] K.H. Hunt and F.R.E. Crossley. Coefficient of restitution interpreted as damping in vibroimpact. *Journal of Applied Mechanics, Trans. ASME*, 42(2):440–445, June 1975.

[11] T.R. Kane and D.A. Levinson. *Dynamics: Theory and Applications*. McGraw-Hill, New York, 1985.

[12] J.B. Keller. Impact with friction. *Journal of Applied Mechanics*, 53:1–4, March 1986.

[13] H.M. Lankarani. Contact force model with hysteresis damping for impact analysis of multibody systems. *ASME, DED*, 19-3(pt 3):45–51, September 1989.

[14] P. Lotstedt. Mechanical systems of rigid bodies subject to unilateral constraints. *SIAM Journal on Applied Mathematics*, 42(2):281–296, April 1982.

[15] F. Pfeiffer and C. Glocker. *Multi-body dynamics with unilateral constraints*. Wiley, New York, 1996.

[16] A. Rodriguez and A. Bowling. Analytic solution to indeterminate impact with friction using stronge's hypothesis. *Multibody System Dynamics (In Review)*, 2012.

[17] I. Sharf and Y. Zhang. A contact force solution for non-colliding contact dynamics simulation. *Multibody System Dynamics*, 16(3):263–290, October 2006.

[18] W.J. Stronge. *Impact Mechanics*. Cambridge University Press, 2000.